Accurate Electromagnetic Transient Modelling of Sector-Shaped Cables

K.K.M.A. Kariyawasam, A. M. Gole, B. Kordi, H.M.J.S.P. De Silva

***Abstract*-- This paper proposes an approach for electromagnetic transient modelling of sector-shaped cables. Frequency dependant resistances and inductances of the cable are obtained using a sub-conductor technique which also includes a representation of the surrounding ground. The elemental sub-conductor technique which normally handles circular shapes is extended to include sector conductor shapes which are generally non-circular. Values obtained are then used to formulate the Z and Y matrices for the cable and the wave propagation characteristics for the natural modes are analyzed. A time domain simulation is carried out using the developed model for an example case.**

***Keywords*: sector-shaped cables, electromagnetic transient modelling, frequency dependant parameters, sub-conductor.**

I. INTRODUCTION

AS a result of environmental and political pressures, underground cables are increasingly being preferred to overhead transmission lines in many European countries. Sector-shaped cables are widely used in modern power systems, especially at low and medium voltage distribution. Their advantage is that they provide a smaller outer diameter for the same conductor cross-section compared to circular conductor shapes due to the uniformity of the insulation layer. However, compared with traditional coaxial cables, the electro-magnetic transient (EMT) modelling of sector shaped-cables is a challenge due to the complexity of finding frequency dependant parameters for such a non-conventional configuration. The aim of this paper is to provide a guideline to model such a cable in EMT-type software.

Frequency dependant resistances and inductances of arbitrary-shaped cables can be calculated using the conductor subdivision method, in which each conductor of the cable is partitioned into a number of small sub-conductors [1]. The shape of the sub-conductor can be circular, square or elemental. However circular and square sub-conductors require a large number of subdivisions to get accurate results, thus requiring significant computational effort and memory [2]. The elemental sub-conductor technique proposed in [2] for cables with circular and coaxial cross-sections, requires a smaller number of subdivisions to reach accurate results.

K. K. M. A. Kariyawasam, A. M. Gole and B. Kordi are with the Dept. of Electrical and Computer Eng., University of Manitoba, Canada (e-mail: kapuge@ee.umanitoba.ca, gole@ee.umanitoba.ca, bkordi@ee.umanitoba.ca).

H.M.J.S.P. De Silva is with the Manitoba HVDC Research Centre, Canada (e-mail: jeewantha@hvdc.ca).

Paper submitted to the International Conference on Power Systems Transients (IPST2011) in Delft, the Netherlands June 14-17, 2011

However, as the conductors of sector-shaped cable are not circular sections (as shown in Fig. 2) the above method cannot be directly used for such cables. This paper presents an approach for applying the elemental sub-conductor technique to sector-shaped cables with only a slight deviation at the circumference which is shown in the paper to be negligible when the number of sub-conductors is chosen properly. Impedance of the ground return path is calculated by subdividing ground into rectangular sub-conductors, size of which change with the frequency. Impedances calculated using this method, are compared with those obtained by closed form approximate formulae provided in [6].

Simplified equations are presented in [3] to calculate capacitances of sector-shaped cables approximately. The approach is validated using a finite element analysis.

For a sector-shaped cable example, the frequency domain characteristics are discussed and propagation modes are analyzed by plotting velocities, attenuation of the modes (e.g. ground mode) as a function of frequency. The parameters obtained are then used to perform time-domain electromagnetic transient simulations of the sector shaped cable system. The EMT-simulation results are verified by simulating a case with linear terminating impedances and comparing the time-domain results with those obtained using a numerical inverse Laplace transform approach.

II. IMPEDANCE CALCULATION

A. Subdivision Procedure

The elemental sub-conductor technique proposed in [2] has been used successfully for circular conductor shapes and is proven ([1] & [2]) to provide better results than square and circular sub-conductor shapes. Subdivision of a circle or an annulus into elemental shaped (Fig. 1 a)) sub-conductors is simple & unambiguous. However, the sectors of a sector-shaped cable are not necessarily circular sections and must be handled differently. This is discussed in detail in this section.

Several factors have to be carefully considered in determining the number of sub-conductors required for each conductor of the cable. In general, the accuracy of the frequency dependent parameters can be improved by increasing the number of sub-conductors. As the frequency increases the resistances obtained using sub-conductor techniques asymptotically reach a “cut-off resistance”, which is slightly higher than the dc resistance of the outermost sub-conductors [2]. This is primarily due to the reduction of skin depth with frequency. Therefore, the applicable frequency range can be increased by selecting small sub-conductor filaments. However this increases the total number of sub-

conductors significantly and there by the computational effort and memory. By exponentially subdividing the conductor as seen in Fig. 1 c), outer sub-conductors can be made smaller (compared to inner sub-conductors) and thereby reducing the total number of sub-conductors [2]. The number of sub-conductor filaments should be selected based on the above facts as well as the accuracy level expected.

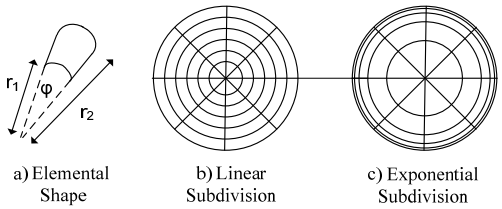

Fig. 1 Elemental Subdivision

Subdivision of the sheath can be performed using the method discussed above. However, the center of the inner conductors (C_0) of a sector shaped cable lies outside the conductor (as seen in Fig. 2), which indicates they are not circular sectors. Hence the following procedure is introduced in this paper to effectively subdivide such conductors.

Initially, each sector-shaped conductor can be subdivided in the azimuth direction at a constant angle, φ. Fig. 2 b) shows an arbitrary sub-sector with an angle, φ and radii at each side being r'_1 & r''_1, both of which can be found using (1). This sub-sector is then replaced with a circular sub-sector with same angle, φ and a constant radius of $(r'_1+ r''_1)/2$, which is an average of the previous radii. This circular sub-sector can be subdivided in the radial direction into conventional "elemental" type sub-conductors.

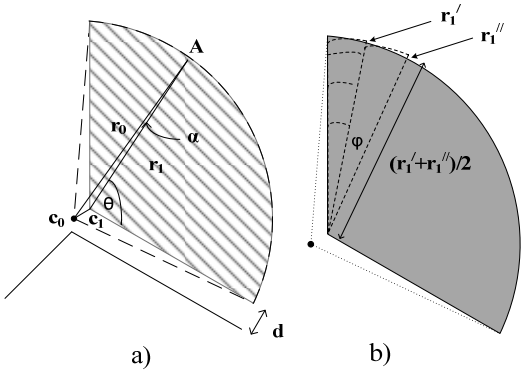

Fig. 2 Subdivision of Sector-shaped Cable

The distance, r_1 from conductor vertex (C_1) to the circumference (A) is not a constant. r_1 at any given angle, θ (in degrees) can be calculated in terms of r_0 and d as,

$$r_1 = \begin{cases} \dfrac{r_0}{\sin\left(120^0+\theta\right)}\sin\left\{60^0-\theta-\alpha\right\}, for\theta \neq 60^0 \\ r_0 - \dfrac{d}{2}\cos\left(30^0\right), for\theta = 60^0 \end{cases} \quad (1)$$

where,

$$\alpha = \sin^{-1}\left[\frac{\frac{d}{2}\cos\left(30^0\right)}{r_0}\sin\left(120^0+\theta\right)\right]$$

Derivation of (1) is given in the Appendix.

B. Use of a Fictitious Return Conductor

The elements of the impedance matrix depend on the return path selected; especially the inductances in which self and mutual Geometric Mean Distances (GMDs) are calculated with respect to loops formed involving the return conductor [2]. A fictitious, lossless and circular ring enclosing the cable is chosen as the return path. Here the effect of the surrounding ground is not considered, as the aim is to facilitate comparisons with the method proposed in [4] & [8].

I. RESISTANCE CALCULATION

Due to the constant current density assumption, within a sub-conductor filament, resistance calculation of any sub-conductor, *i* can be performed using the cross-sectional area of that sub-conductor, A_i and the resistivity, ρ of the corresponding conductor as shown below.

$$R_i = \frac{\rho}{A_i} \quad (2)$$

A_i is given by,

$$A_i = \frac{(r_{2i}^2 - r_{1i}^2)}{2}\varphi \quad (3)$$

Where, r_{1i} and r_{2i} are the minimum and maximum radii of the sub-conductor, and φ is the sub-sector angle (in radian) as seen in Fig. 1 a).

II. INDUCTANCE CALCULATION

Obtaining self and mutual GMDs of sub-conductors is necessary prior to the calculation the inductances. Formulae needed for GMD calculation are given in [2] and thus, not repeated.

For a return conductor being a ring with radius a, the self GMD of the i^{th} sub-conductor is GMD_i and the mutual GMD between the i^{th} and j^{th} sub-conductors is GMD_{ij}. The inductances can be found as follows [4];

$$L_{ii} = \frac{\mu}{2\pi}\ln\left(\frac{a}{GMD_i}\right) \quad (4)$$

$$L_{ij} = \frac{\mu}{2\pi}\ln\left(\frac{a}{GMD_{ij}}\right) \quad (5)$$

III. MATRIX REDUCTION

Assuming the number of conductors (including the sheath) to be k, and the number of sub-conductors in each conductor to be N making the number of total sub-conductors n = N x k. The number N is taken to be constant for all conductors in following analysis to simplify the discussion. However, the generalized procedure considers cases with different number of sub-conductors in each conductor. The sub-conductor

impedance matrix at a frequency, f can be written as,

$$Z_{n\times n}(f)=\begin{bmatrix} R_1 & 0 & \cdots & 0 \\ 0 & R_2 & & \vdots \\ \vdots & & \ddots & \vdots \\ 0 & \cdots & \cdots & R_n \end{bmatrix}+j2\pi f\begin{bmatrix} L_{11} & L_{12} & \cdots & L_{1n} \\ L_{21} & L_{22} & & \vdots \\ \vdots & & \ddots & \vdots \\ L_{n1} & \cdots & \cdots & L_{nn} \end{bmatrix} \quad (6)$$

This Z(f) matrix relates to the voltage and the sub-conductor current as;

$$-\frac{d}{dx}\left[V_{n\times 1}\right]=Z_{n\times n}\left[I_{n\times 1}\right] \quad (7)$$

By inverting Z(f),

$$-\begin{bmatrix} I_1^1 \\ I_2^1 \\ \vdots \\ I_N^1 \\ I_{N+1}^2 \\ \vdots \\ \vdots \\ I_n^k \end{bmatrix}=\begin{bmatrix} Y_{11} & Y_{12} & \cdots & Y_{1N} & Y_{1(N+1)} & \cdots & \cdots & Y_{1n} \\ Y_{21} & Y_{22} & & \vdots & & & & \vdots \\ \vdots & & & \vdots & & & & \vdots \\ Y_{N1} & \cdots & \cdots & Y_{NN} & & & & \\ Y_{(N+1)1} & \cdots & \cdots & \cdots & Y_{(N+1)(N+1)} & & & \\ \vdots & & & & & & & \\ \vdots & & & & & & & \vdots \\ Y_{n1} & \cdots & \cdots & & & & \cdots & Y_{nn} \end{bmatrix}\frac{d}{dx}\begin{bmatrix} V^1 \\ V^1 \\ \vdots \\ V^1 \\ V^2 \\ \vdots \\ \vdots \\ V^k \end{bmatrix} \quad (8)$$

The superscripted number represents the conductor number and the subscripted numbers represent sub-conductors. It can be observed that first N voltages are the same (V^1) as they belong to the same conductor and the next N to the second conductor. Therefore, the addition of currents I_1^1 to I_N^1 would give the conductor 1 current and the currents I_{N+1}^2 to I_{2N}^2 would give the conductor 2 current and so on. This would yield a reduced Y matrix of size k×k;

$$-\begin{bmatrix} I_1 \\ \vdots \\ I_k \end{bmatrix}=\begin{bmatrix} Y_{sum\_11} & Y_{sum\_12} & \cdots & Y_{sum\_1k} \\ \vdots & Y_{sum\_22} & \ddots & \vdots \\ Y_{sum\_k1} & \cdots & \cdots & Y_{sum\_kk} \end{bmatrix}\frac{d}{dx}\begin{bmatrix} V_1 \\ \vdots \\ V_k \end{bmatrix} \quad (9)$$

The subscripts m and r denote m^{th} and r^{th} conductor,

$$I_m=I^m_{(m-1)N+1}+I^m_{(m-1)N+2}+\cdots+I^m_{mN}$$

$$Y_{sum\_mm}=\left(Y_{(m-1)N\times(m-1)N}+\cdots+Y_{(m-1)N\times mN}\right)+\cdots$$
$$\cdots+\left(Y^m_{mN\times(m-1)N}+\cdots+Y^m_{mN\times mN}\right)$$

$$Y_{sum\_mr}=\left(Y_{(m-1)N\times(r-1)N}+\cdots+Y_{(m-1)N\times rN}\right)+\cdots$$
$$\cdots+\left(Y_{mN\times(r-1)N}+\cdots+Y_{mN\times rN}\right)$$

By inverting Y(f) matrix in (9),

$$-\frac{d}{dx}\left[V_{k\times 1}\right]=Z_{k\times k}\left[I_{k\times 1}\right] \quad (10)$$

Although simple, this procedure requires the inversion of an n×n matrix which may be difficult for large number of subdivisions. Matrix reduction methods discussed in [1] & [2] can be applied to improve computational efficiency.

A. Inclusion of ground

In the approach proposed in this paper, the ground in which the cable is buried is also accomplished by subdivision of the surrounding ground into sub-conductor filaments, similar to what was done earlier for the conductor. However, if constant sub-conductor size is used, large skin depth at low frequencies poses a problem due to large number of sub-conductors. In the frequency range of 1Hz-1MHz, skin depth can vary from 5m to 5000m at a typical earth resistivity of 100 Ωm. Therefore, subdivision of ground was carried out depending on the skin depth at each frequency. The number of total sub-conductors used was kept constant and the sub-conductor size is varied depending on the frequency (as shown in Fig. 3). However, sub-conductor size was kept constant and comparatively small near the earth surface and the cable as higher current density variation is expected there. A square shaped area with side length of twice the skin depth is considered for the subdivision and square shaped sub-conductors are used.

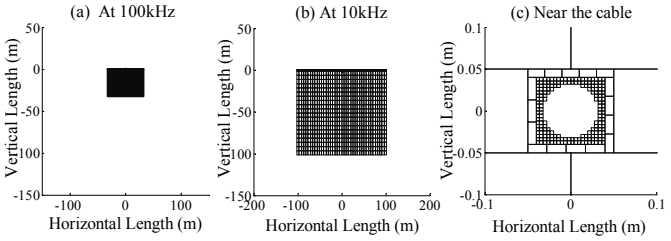

Fig. 3 Subdivision of ground

An alternate method for the inclusion of ground is by using approximate formulae for earth return impedance given in [5] & [6]. The formula proposed in [6] for self earth return impedance is as follows;

$$Z_s=\frac{\rho m^2}{2\pi}\left[K_0(mR)+\frac{2}{4+m^2R^2}e^{-2hm}\right] \quad (11)$$

Where ρ is resistivity of earth, R is the outer radius of the cable, h is the depth of the cable and γ is the Euler constant. The intrinsic propagation constant of the earth, m, given by $m = \sqrt{(j\omega\mu/\rho)}$. The impedance matrix obtained can be modified as in [1] to include the earth return impedance as follows;

$$Z_{ij\_new}=Z_{ij\_old}-Z_{ref}+Z_{ground}+Z_{insulation} \quad (12)$$

Z_{ground} can be found from (11) and Z_{ref} can be found by considering the whole cable as an "elemental" and using equation (4). $Z_{insulation}$ is given as,

$$Z_{insulation}=\frac{j\omega\mu}{2\pi}\ln\left(\frac{Outer\ radius\ of\ insulation}{Inner\ radius\ of\ insulation}\right) \quad (13)$$

III. CASE STUDY

A sector-shaped cable studied in [4] and [7] (shown in Fig. 4) is used for the impedance value calculation.

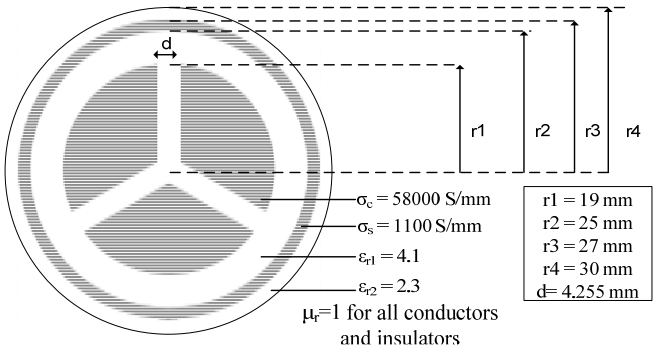

Fig. 4 Geometry of the Sector-shaped Cable

Resistances and inductances calculated with respect to a reference conductor are compared with the finite element analysis of the same cable provided in [8] for six frequencies ranging from 6 to 600 kHz. A total of 1920 sub-conductors are used for the calculation. Comparisons of self and mutual resistances and inductances are given in Tables I to IV.

All four parameters seem to match acceptably with the finite element results. It can be noted that percentage difference in the two methods increase with the frequency. This can be due to the increase in sub-conductor width compared to the skin depth.

TABLE I
SELF RESISTANCE COMPARISON

Frequency (Hz)	Resistance (Ω/km)		Difference (%)
	Finite Element method	Sub-conductor Method	
6	2.8400	2.8400	0.000
60	2.8499	2.8499	0.000
600	2.9675	2.9608	0.225
6E+03	3.5250	3.5076	0.493
60E+03	5.1505	5.2022	-1.000
600E+03	15.916	14.767	7.220

TABLE II
MUTUAL RESISTANCE COMPARISON

Frequency (Hz)	Resistance (Ω/km)		Difference (%)
	Finite Element method	Sub-conductor Method	
6	2.7825	2.7824	0.003
60	2.7832	2.7833	-0.003
600	2.7804	2.7871	-0.241
6E+03	2.6946	2.7090	-0.534
60E+03	2.8882	2.7693	4.110
600E+03	8.8231	7.9854	9.490

TABLE III
SELF INDUCTANCE COMPARISON

Frequency (Hz)	Inductance (μH/km)		Difference (%)
	Finite Element method	Sub-conductor Method	
6	232.02	229.98	0.91
60	220.67	218.32	1.13
600	156.80	155.35	0.78
6E+03	120.40	121.61	1.19
60E+03	105.09	107.42	-2.49
600E+03	99.003	102.81	-4.60

TABLE IV
MUTUAL INDUCTANCE COMPARISON

Frequency (Hz)	Inductance (μH/km)		Difference (%)
	Finite Element method	Sub-conductor Method	
6	40.445	40.833	-0.959
60	40.191	40.207	-0.039
600	35.722	34.627	3.060
6E+03	38.324	35.607	7.080
60E+03	40.692	37.524	7.780
600E+03	38.061	34.661	8.930

Impedances were calculated for the same cable with respect to ground using both ground subdivision and approximate formulae. The corresponding plots of all parameters are shown in Fig. 5 and 6. Earth resistivity is assumed to be 100 Ωm. An additional 1278 sub-conductors were introduced in the ground subdivision method, which increased the total number of sub-conductors to 3198.

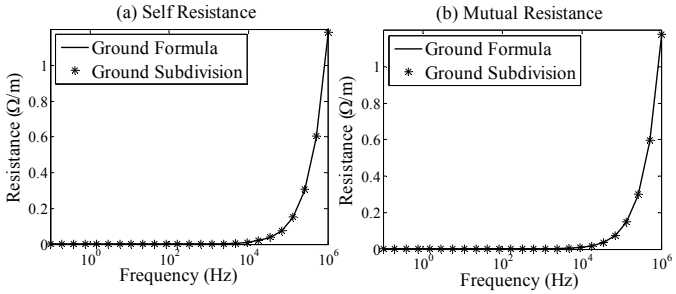

Fig. 5 Resistances after ground inclusion

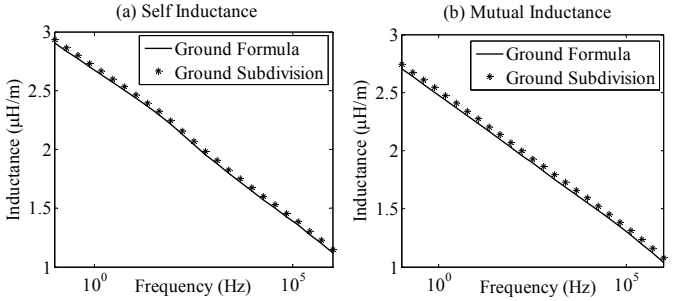

Fig. 6 Inductances after ground inclusion

It is observed in Fig. 5 and 6 that the resistance and inductance values obtained from both methods agree satisfactorily. This shows that the use of formula (11) gives an accurate value for the ground, and that the more detailed sub-conductor method could be avoided when considering ground.

III. CAPACITANCE CALCULATION

Unlike resistances and inductances, capacitance values do not change noticeably within the frequency range (up to 1 MHz) considered. Therefore, capacitance values obtained at a single frequency can be used for all frequencies without loss of much accuracy.

Capacitance values are attained by a full-wave analysis in [9] of the cable shown in Fig. 4 using finite element software (Comsol Multiphysics). These values compared well with the results from approximate method proposed in [3]. For a cable

with three sectors, capacitance matrix is as follows;

$$C = \begin{bmatrix} 2C_c + C_s & -C_c & -C_c & -C_s \\ -C_c & 2C_c + C_s & -C_c & -C_s \\ -C_c & -C_c & 2C_c + C_s & -C_s \\ -C_s & -C_s & -C_s & 3C_c + C_g \end{bmatrix} \quad (14)$$

Where,

$$C_c = \frac{\varepsilon r_1}{d} \quad C_s = \frac{2\pi\varepsilon}{3\ln\left(\frac{r_2}{r_1}\right)} \quad C_g = \frac{2\pi\varepsilon}{\ln\left(\frac{r_4}{r_3}\right)}$$

Radii, r_1 to r_4 and d are shown in Fig. 4. Comparison of the capacitances using the software model at 800 kHz and 1 MHz and the above method is given in Table V.

TABLE V
CAPACITANCE VALUE COMPARISON

Elements of Capacitance Matrix	From Comsol at 800 kHz (nF)	From Comsol at 1 MHz (nF)	Approximate Method (nF)
C_{11}	603.73	595.91	601.23
C_{14}	-277.21	-272.88	-277.04
C_{23}	-160.68	-159.79	-162.10
C_{44}	201.00	195.45	204.55

It can be seen the approximate capacitance values are in a close agreement with that from software as the maximum difference in the values obtaining from the two methods is 4.45%.

IV. FREQUENCY DOMAIN ANALYSIS

R, L and C values for the cable are calculated according to the procedures mentioned in sections II and IV. The effect of shunt conductance is assumed to be very small and therefore neglected. It is then possible to formulate Z and Y matrices for the cable at any frequency up to 1 MHz. Once Z and Y are known propagation coefficients of the four natural modes are given by the eigen values of √(ZY). Then, the attenuations and Mode Velocities for the modes can be found as follows;

$$\text{Attenuation Coefficient, } \alpha = \text{Re}\{\gamma\} \quad (15)$$

$$\text{Phase Coefficient, } \beta = \text{Im}\{\gamma\}$$

$$\text{Mode Velocity, } v = \frac{\omega}{\beta} \quad (16)$$

Where γ is propagation coefficient and ω is frequency in rad/s. Then, Attenuation and mode Velocity of all the nodes are plotted against frequency in Fig. 7 and 8.

The mode distribution vector for current at 1 MHz is shown in Table VI. Mode 'a' can be identified as a zero sequence mode with relatively high attenuation and very low velocity. Mode 'b' (sheath to conductor mode) is energized by injecting a current into sheath and extracting it from inner three conductors. Mode 'c' and'd' can be identified as inter-conductor modes as their modal attenuation and velocity characteristics are almost identical.

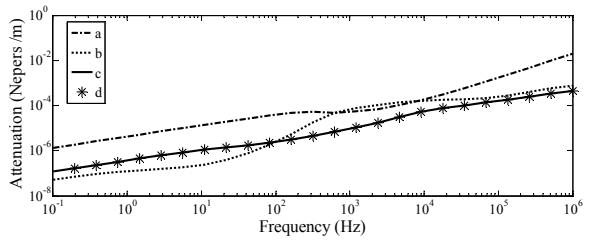

Fig. 7 Attenuation Characteristics of Modes

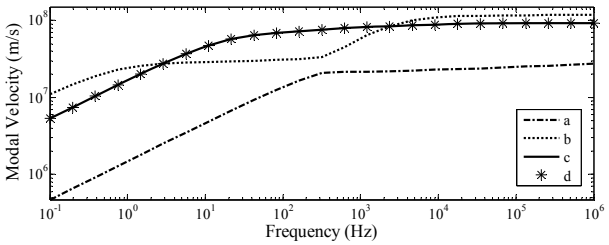

Fig. 8 Velocity Characteristics of Modes

TABLE VI
MODE DISTRIBUTION VECTORS FOR CURRENT

Mode	a	b	c	d
Attenuation (dB/m)	0.1739	0.0054	0.0025	0.0025
Velocity (km/ms)	28.399	118.85	92.528	92.532
Conductor 1	0.0000	-0.2884	0.7776	-0.2480
Conductor 2	0.0000	-0.2886	-0.6029	-0.5494
Conductor 3	0.0000	-0.2889	-0.1744	0.7971
Sheath	1.0000	0.8661	-0.0003	-0.0003

V. TIME DOMAIN SIMULATION

Once both Z and Y matrices are known, Admittance and propagation characteristics are fitted with rational functions using the method of vector fitting [10] in EMT-type software (PSCAD/EMTDC) and a time domain simulation is carried out with the termination network shown in Fig. 9.

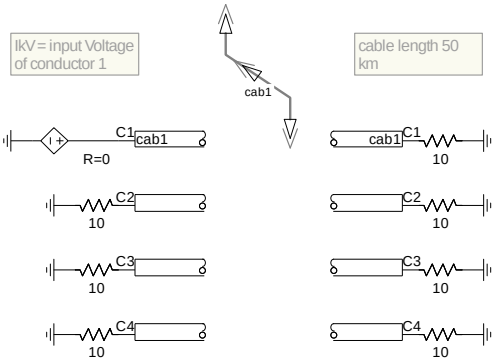

Fig. 9 Implementation in PSCAD/EMTDC

Inner conductors are denoted by C_1, C_2 and C_3 and sheath by C_4. Conductor, C_1 is energized with a 1 kV Voltage step. Then, the sending end current is observed and compared with the results obtained using Numerical Inverse Laplace Transform (NILT) [11] of the frequency domain equations.

Fig. 10 shows the two methods are in close agreement, thereby confirming that the time domain model is accurate.

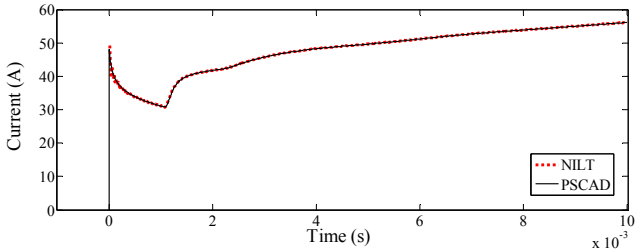

Fig. 10 Sending End Current

VI. CONCLUSION

A simple approach based on sub-conductor technique is proposed to calculate frequency dependant resistances and inductances of a Sector-shaped cable. The validity of the method was confirmed using comparison with finite element modelling. The surrounding ground in which the cable is embedded can be accounted for by including a conduction region whose size is varied according to penetration distance at the frequency of interest. This region is further divided into sub-conductor filaments. Comparison with an alternate approach using approximate equations indicated that the approximate equations are adequate in describing the effect of ground and hence greatly reduce the computational burden compared to that of a sub-conductor division of the ground. Once the parameters are obtained, a frequency domain analysis was conducted to determine the characteristics of the natural modes of the cable such as mode propagation velocity and mode attenuation as functions of frequency. The cable's impedance and admittance matrices were also fitted with rational functions and included in a time-domain simulation. The time-domain simulation was validated by comparison with an inverse-Laplace solution. This confirms that sector-shaped cables can now be accurately modelled in the frequency and time domains.

VII. APPENDIX

Here, we consider finding r_1 shown in Fig. 2 a) using the known values of r_0, d and θ.

A. For $\theta \neq 60^0$

In this case, points A, C_0 and C_1 form a triangle. Lets denote $C_0\hat{A}C_1$ angle to be α.

$C_0C_1 = \frac{d}{2}\cos(30^0)$, as each sector is 120^0

Then, by applying sine law to C_0AC_1,

$$\frac{\frac{d}{2}\cos(30^0)}{\sin(\alpha)} = \frac{r_0}{\sin(120^0+\theta)} = \frac{r_1}{\sin(60^0-\theta-\alpha)} \qquad (17)$$

This gives,

$$\alpha = \sin^{-1}\left[\frac{\frac{d}{2}\cos(30^0)}{r_0}\sin(120^0+\theta)\right]$$

This gives,

$$r_1 = \frac{r_0}{\sin(120^0+\theta)}\sin(60^0-\theta-\alpha) \qquad (18)$$

B. For $\theta = 60^0$

In this case, points A, C_0 and C_1 become collinear. Therefore,

$$r_1 = r_0 - C_0C_1$$
$$r_1 = r_0 - \frac{d}{2}\cos(30^0) \qquad (19)$$

VIII. REFERENCES

[1] P. de Arizón and H. W. Dommel, "Computation of cable impedances based on subdivision of conductors", *IEEE Transactions on Power Delivery,* vol. 2, pp. 21–27, Jan. 1987.

[2] R. Lucas and S. Talukdar, "Advances in finite element techniques for calculating cable resistances and inductances", *IEEE Transactions on Power Apparatus and Systems,* vol. 3, pp. 875-883, May/June 1978.

[3] J. Dickinson and P.J. Nicholson, "Calculating the high frequency transmission line parameters of power cables", *ISPCLA ESSEN, Apr. 1997,* pp. 127-133.

[4] R. A Rivas, J. R. Marti, "Calculation of Frequency-Dependant Parameters of Power Cables: Matrix Partitioning Techniques", *IEEE Transactions on Power Delivery*, vol. 7, pp. 1085-1092, Oct. 2002.

[5] L. M. Wedepohl, D. J. Wilcox, "Transient analysis of underground power-transmission systems-System-model and wave-propagation characteristics", *in Proc. Of Institute of Electrical Engineers*, vol. 120, pp. 253-260, feb. 1973.

[6] O. Saad, G. Gaba, M. Giroux, "A Closed-Form Approximation for Ground Return Impedence of Underground Cables", *IEEE Transactions on Power Delivery,* vol. 11, pp. 1536–1545, Jul. 1996.

[7] A. Ametani, K. Fuse, "Approximate method for calculating the impedances of multiconductor cross section of arbitrary shapes", Elect. Eng. Japan, vol. 112, no 2, pp. 117-123, 1992.

[8] R. Rivas, "Calculation of Frequency-Dependant Parameters of Power Cables with Digital Imaging and Partial Subconductors", Ph.D. dissertation, Dept. of Elect. & Comp. Eng., Univ. British Columbia, July 2001.

[9] S. Habib, B. Kordi, "Calculation of Underground Cables Frequency-Dependent Parameters Using Full-Wave Modal Analysis", *International Conference on Power Systems Transients*, Delft, Netherlands June 2011-submitted.

[10] Morched, B. Gustavsen, M. Tartibi, "A universal model for accurate calculation of electromagnetic transients on overhead lines and underground cables", *IEEE Transactions on Power Delivery*, vol.14, no.3, pp.1032-1038, Jul 1999.

[11] L.M Wedepohl, "Transmission Line Theory", Course Notes.